JOURNAL OF MATERIALS SCIENCE **36** (2001) 3355 – 3363

The poly(ethylene terephthalate)/polyaniline composite: AFM, DRS and EPR investigations of some doping effects

A. A. PUD
Institute of Bioorganic Chemistry and Petrochemistry, National Academy of Sciences of Ukraine, 50 Kharkovskoye Shosse, Kiev, 253160, Ukraine

M. TABELLOUT*, A. KASSIBA, A. A. KORZHENKO
Laboratoire de Physique de l'Etat Condensé, UPRES CNRS 6087, Universite du Maine, Avenue O. Messiaen, 72087 Le Mans, Cedex 9, France
E-mail: mohamed.tabellout@univ-lemans.fr

S. P. ROGALSKY, G. S. SHAPOVAL
Institute of Bioorganic Chemistry and Petrochemistry, National Academy of Sciences of Ukraine, 50 Kharkovskoye Shosse, Kiev, 253160, Ukraine

F. HOUZÉ, O. SCHNEEGANS
Laboratoire de Genie Electrique de Paris, UMR CNRS 8507, Supélec, Universités Paris VI et Paris XI, rue Joliot Curie, 91192 Gif-sur-Yvette Cedex, France

J. R. EMERY
Laboratoire de Physique de l'Etat Condensé, UPRES CNRS 6087, Universite du Maine, Avenue O. Messiaen, 72087 Le Mans, Cedex 9, France

A composite based on PET as a matrix and a thin layer of PANI produced by chemical polymerisation of aniline in the surface layer of the PET is investigated by means of four probe conductivity method, standard and conducting AFM, DRS and EPR techniques. Conducting AFM shows that PANI forms conducting clusters. Standard AFM topographical images prove that the undoped form of the composite has a flat surface, whereas the doped one exhibits mountainous features. DRS spectra revealed that the transition from the undoped form to the doped one is accompanied with an increase of the high frequency peak associated to conductivity of the clusters leading to the appearance of two low frequency relaxation processes connected with interfacial polarization phenomena. It is found that the relaxation behaviors of the composite doped by $HClO_4$ and HCl acids are similar. The EPR spectra obtained in both doped and undoped forms of the composite are induced by two kinds of paramagnetic centres (PC). Irrespective to the dopant, anomalous thermal behaviors of the PC spin relaxation times and susceptibilities are evidenced above 180 K. These effects are connected with changes in the electronic transport properties.

1. Introduction

A necessity to overcome problems of poor mechanical properties and processing of conducting polymers gave rise to various approaches, one of the best is probably the creation of composite materials involving both conducting and common polymers [1, 2]. In its turn, this resulted in the development of many kinds of such materials having different composition, structure, and being homogeneous or heterogeneous, etc., which offered a variety of properties and practical applications [3]. It is clear that one of the main factors effecting the conductive properties of the composite is a physical-chemical interaction (e.g. hydrogen bonding, orientation of a monomer at a formation stage) between the monomer units of conducting polymer and the matrix polymer [2, 4]. It was shown, recently, that such an interaction resulted in a strong dependence of the possibility of aniline redox-polymerization inside a common polymer matrix on the nature of the polymer and of the oxidant [4]. Specifically, it was found possible for the system including poly(ethylene terephthalate) (PET) as matrix (swelled by aniline) and HOCl (attendant in Cl_2

* Author to whom all correspondence should be addressed.

water solution or even in HCl and ammonium persulphate solution) as oxidant [4]. As a consequence, a new transparent two layer PET/polyaniline composite with surface conductivity and sensor properties was developed [4, 5]. The first layer of this material consists of polyaniline distributed inside a thin layer (∼1–2 μm) of a PET matrix. It is cohesively connected with a second pure PET layer of the matrix [4].

Recently, it was shown by dielectric relaxation spectroscopy (DRS) that this composite in its conducting form (e.g. when polyaniline (PANI) was doped by HCl) gives two relaxation processes, which are absent in the case of the undoped form [6]. The origin of these processes and their relation to condition of PANI in the composite was not fully understood, but it was suggested that charge carriers are responsible for these phenomena. In this work we try to explain them using additional data mainly of DRS, EPR spectroscopy, atomic force microscopy (AFM) and dc conductivity measurements.

2. Experimental

2.1. Materials

The PET bi-axially stretched films with crystallinity degree ∼70% and thickness 20 μm (Goodfellow Cambridge Ltd) were used as a matrix polymer to produce the PET/PANI film composite. For this aim the films were swelled up to 10 wt. % contents of aniline and were further immersed into the chlorine containing oxidant solution in accord with refs [4, 5]. The final composite film consisted of two layers. The first one, with thickness approximately 1–2 μm estimated by Raman Spectroscopy [5], was practically the composite material containing polyaniline distributed inside PET matrix [4]. The second one was pure PET. Doping of the PET/PANI composite by HCl was performed in a dryer in HCl atmosphere over 37% fuming acid for 0.5 h. Doping the PET/PANI composite by $HClO_4$ was performed in 20% $HClO_4$ water solution for 48 h. No degradation of the composite was observed. Dedoping of the composite was performed by its treatment in the 5 wt% NH_4OH water solution for 2 h. A 24 h treatment gave the same results. The completeness of the dedoping and doping was controlled performing dc-conductivity measurements by the four probe method.

2.2. AFM measurements

AFM measurements were performed with a Nanoscoper® III Multimode™ system (Digital Instruments). Standard topographical images were obtained using the TappingMode™ which consists in scanning the sample surface with an oscillating tip slightly tapping the surface. This allows to eliminate frictional forces and proves to be particularly effective on organic materials. Besides conventional height maps, local electrical measurements were carried out in contact mode with an home-built extension of the Nanoscope called "Resiscope". A schematic view of the experimental set-up is sketched in Fig. 1. The left part of the diagram corresponds to the standard AFM, the right part shows the Resiscope extension, requiring of course a conducting probe. Sample and probe holders are carefully insulated from the apparatus frame. When the tip is brought into contact with the sample at a given normal force (typically between 5 nN and 50 nN), a dc bias voltage is applied in the range (−1 V, +1 V). As the sample surface is scanned line after line, a feedback loop keeps the normal force constant and the local current values are measured, converted into resistance values and recorded simultaneously to height data. For all experiments reported here the Resiscope was operated in ambient atmosphere using commercial probes made of n-doped silicon coated with p-doped diamond from Nanosensors GmbH. It must be noted that the high values found for the tip/sample resistance are due to the tiny size of the contact area.

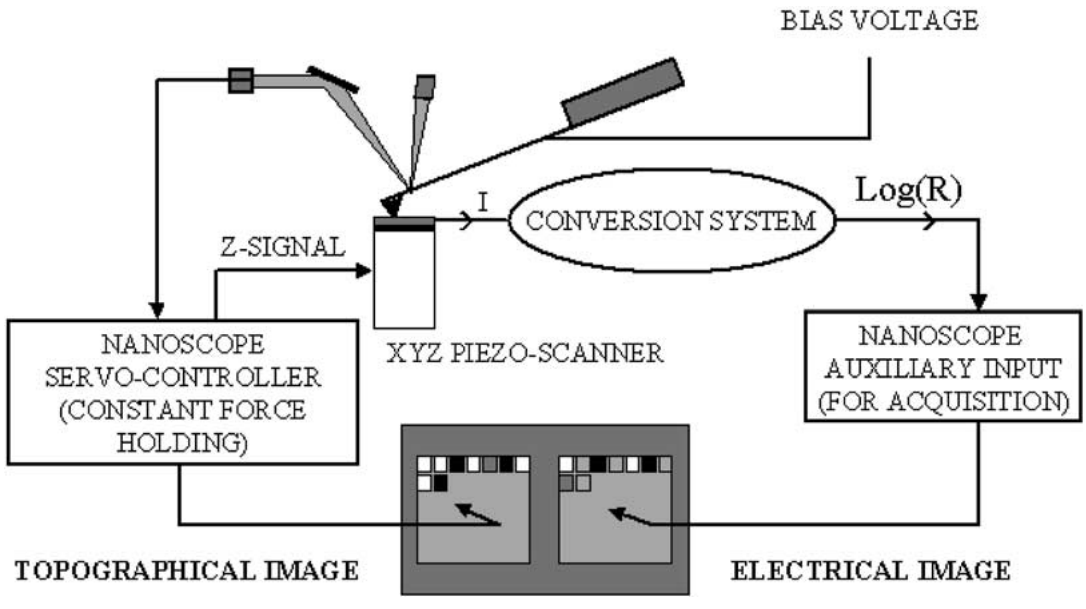

Figure 1 Schematic principle of the Resiscope technique derived from classical AFM.

2.3. DRS measurements

Dielectric relaxation spectra were obtained using a Broadband Dielectric Spectrometer (Novocontrol GmbH) in the frequency range 0.1 Hz to 10 MHz at temperatures from 153 K to 353 K. Precision of the temperature stabilization was ±0.1 K.

In order to quantify the mean relaxation time in the range of present interest the frequency domain permittivity analysis was the method of choice. The real and imaginary dielectric permittivity $\varepsilon^*(\omega) = \varepsilon' - i\varepsilon''$ were fitted by the Havriliak-Negami (HN) function [7]:

$$\varepsilon^*(\omega) = \varepsilon_\infty + \frac{\Delta\varepsilon}{(1 + (i\omega/\omega_O)^\alpha)^\beta} + \frac{\sigma_0}{i\varepsilon_0\omega^n}$$

where $\omega = 2\pi f$; ε_0 denotes the vacuum permittivity, σ_0 the dc conductivity; n an exponential factor, in most cases equal to 1; $\Delta\varepsilon$ is the difference between the low and high frequency limits of ε' over the relaxation to which the HN function applies; $\Delta\varepsilon$ is also proportional to the area below the ε'' relaxation peak; ε_∞ is the unrelaxed value of permittivity; α and β shape parameters. Fitting of the experimental dielectric spectra $\varepsilon^*(\omega)$ was made with WinFit 2.4 (1996) software of Novocontrol GmbH.

The temperature dependencies of the characteristic relaxation times of the different processes were analyzed using the well known Arrhenius law:

$$\tau = \tau_0 \exp\left(\frac{E}{kT}\right)$$

where τ_0 is the relaxation time at very high temperature, E the activation energy and k the Boltzman constant. The relaxation time used is the one obtained by fitting the spectra to the HN function.

The activation energies of the different processes have been obtained by fitting the characteristic relaxation times.

2.4. EPR measurements

EPR investigations were carried out by using a Bruker spectrometer equipped with an X-band ($\nu = 9.45$ GHz). Using a Nitrogen flux with a suitable regulation close to the sample, we performed variable temperature measurements 100 K $\leq T \leq$ 300 K; the temperature uncertainty was within ±0.2 K. During the EPR experiments on the PANI/PET films, a minimum delay time (15 min) at fixed temperature was allowed in order to prevent any kinetic effects connected with mechanical contractions or internal strains induced by cooling the sample. Reversible results were obtained both in the cooling and heating run. So, we limited the forthcoming report to only the cooling run for all the investigated samples. Furthermore, due to the high concentration of paramagnetic centers in the samples, a low microwave power was used (≤2 mW) and a small amplitude of the modulation field (≤0.5 gauss). This suppressed any effect of line shape distortions connected with saturation phenomena. 2,2-Diphenyl-1-picrylhydazil hydrate (dpph) was used as a reference sample with g-factor 2.0036.

3. Results and discussion

It follows from preliminary data [6], that embedding PANI into a thin surface layer of a PET matrix (thickness approximately 5–10% of overall thickness of the composite [4]) changes significantly its dielectric properties. It is obvious that to some extent this can be connected to the specific interaction established earlier (for example, formation of hydrogen bonds) between PANI and PET [4]. However, it seems that charge carriers which are even present in an undoped form of the composite (PET/PANI) have a much more important contribution here. Indeed, a virgin PET has dc surface conductivity about 10^{-13} S/cm but PET/PANI is characterized by much greater magnitude of this parameter 2.3×10^{-10} S/cm. The doping results in its growth for five orders of magnitude up to 9.1×10^{-6} S/cm in the case of HClO4 and up to 1.8×10^{-5} S/cm in the case of HCl. Even these elementary data allow assuming changes of the nature and the degree of PANI interaction with the matrix in the presence of a doping agent.

3.1. AFM investigation

The 3D-AFM technique allowed us to clearly bring to the fore the influence of the dopant on the morphology of the composite surface, which contained polyaniline distributed inside PET matrix. As one can see from topographical Tapping Mode images of Fig. 2, recorded at a relatively high magnification (1.5 μm × 1.5 μm), both the virgin PET and the undoped form of the composite PET/PANI exhibit comparatively flat surfaces, whereas doping leads to the emergence of mountainous features. The effect of the dopant size and its nature on the surface morphology is hence evidenced. Specifically, $HClO_4$ induces the much stronger changes in comparison with the HCl case (see above) though dc conductivity of PET/PANI·$HClO_4$ is only twice lower in all. It allows us to assume that a reason for such an important change in the relief could be due, not only, to the appearance of charge carriers on PANI macromolecules, but also to a distribution of counter-anions compensating their charges in a conducting surface layer of the composite. In particular, it is possible to believe that this effect is caused by a new packing of the amorphous part of PET and PANI which is induced by Cl^- and ClO_4^- anions penetration. In the undoped form PANI fills the less dense volume preferentially near flexible chains of PET. Obviously, larger ClO_4^- anions, when penetrating into the polymer matrix, deform it stronger than Cl^- ones. Besides, the Coulomb repulsion among charged fragments of PANI chains, which are not completely shielded by counter-anions, can also be considered as deforming factor.

The degree of the surface deformation and its shape can essentially be influenced by a non-uniform distribution of PANI in the surface layer of the matrix. As a consequence, clusters with various conductivity values exist in this layer. This specific point was confirmed by Resiscope investigations on the surface of the PET/PANI·$HClO_4$ sample (Fig. 3). The electrical image (right part of the figure) reveals the presence of clusters on which values of the local contact resistance range

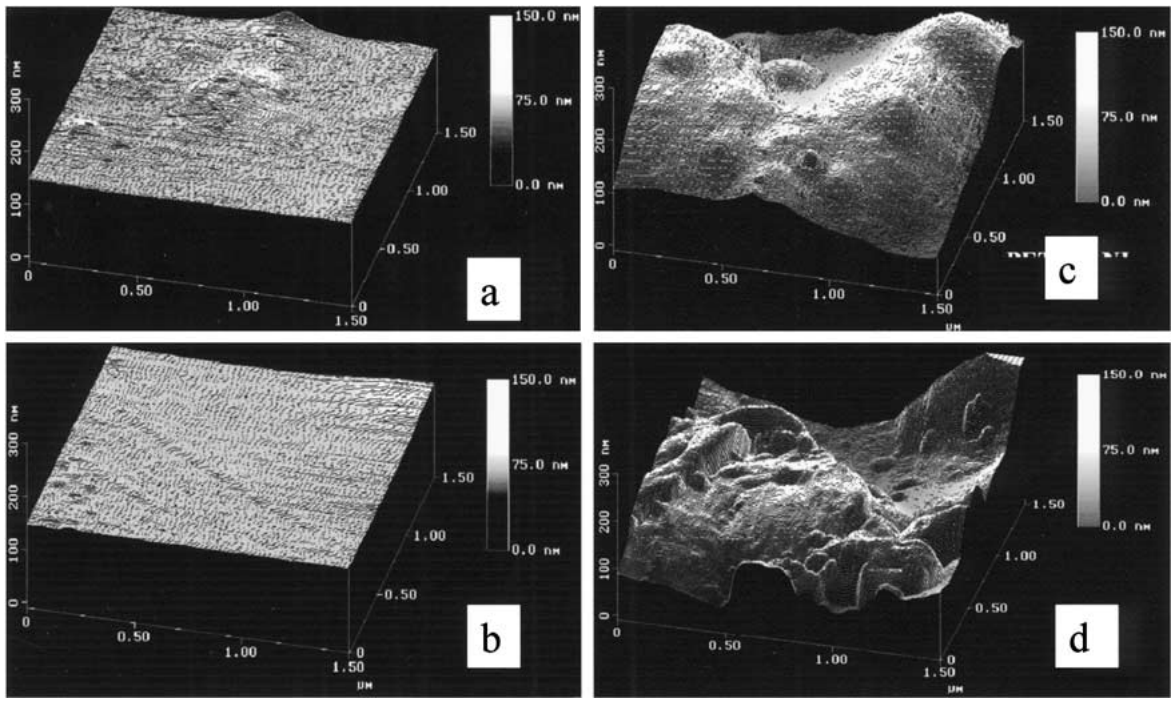

Figure 2 3D-AFM topographical images (TappingMode) of pure PET (a) and the PET/PANI composite: (b) the undoped form; (c) the PET/PANI·HCl form; (d) the PET/PANI·$HClO_4$ form.

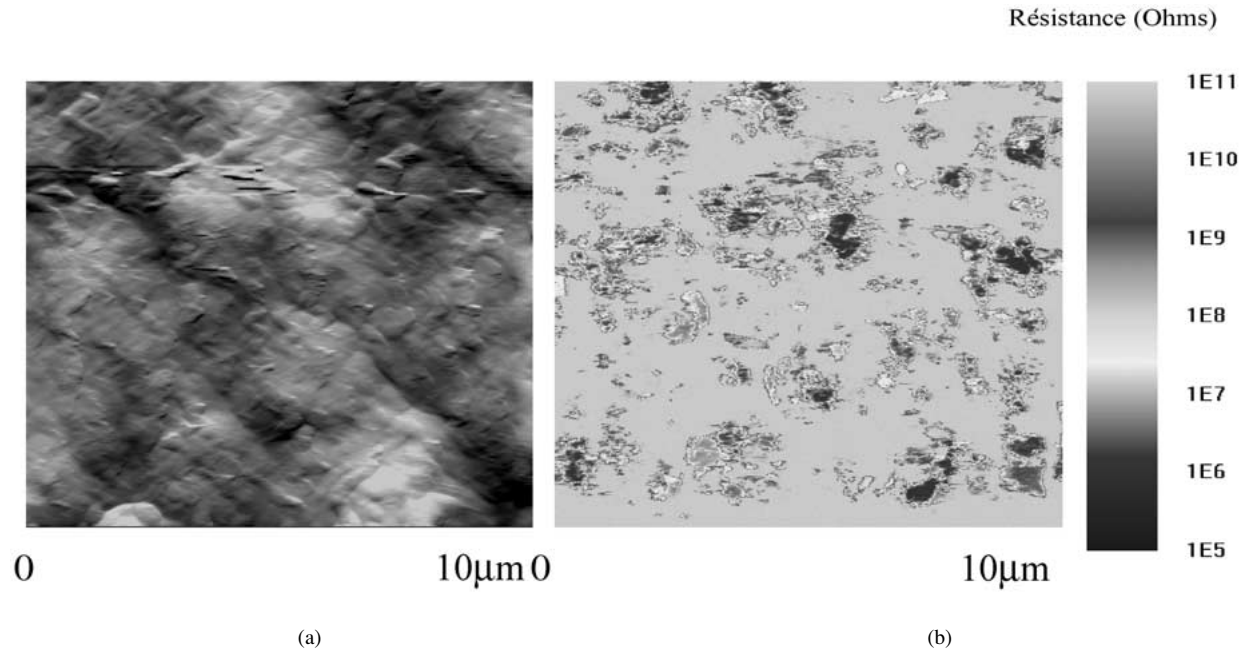

Figure 3 Topographical (a) and electrical (b) AFM images of the surface obtained with the "Resiscope" in contact mode (dc bias of +1 V, normal load of 20 nN).

from $10^5\ \Omega$ to $10^{11}\ \Omega$. It is evident that these clusters are different by shape and can be irregularly distributed in the layer containing PANI leading to a mountainous shape of the surface layer (Figs 2c, and d and 3a). As an indirect confirmation to this, the difficulties in obtaining electrical images of the surface were somewhat unexpected for us. Thus, the first Resiscope scan on the surface with the minimum normal load (about 5 nN) of the probe did not reveal any conducting cluster on the composite surface. Only subsequent scans at a stronger load (10–20 nN), slightly eroding the top layer, allowed to get a conductivity map such as the one presented in Fig. 3. Taking into account the 3D AFM topographical image (Fig. 1), this suggests that the minimally loaded probe contacts only the "upper surface" of the sample. The absence of conductivity suggests that either PANI is absent at this "upper surface", or it is in an overoxidized non-conducting state. The latter possibility seems to us the most probable, since in the conditions of aniline redox polymerization in the PET matrix the surface layer is constantly subjected to the action of an oxidizer [4] and can therefore be overoxidized [8].

As a whole, the AFM data testify to a significant phase segregation revealed by clusters of various conductivity in the thin surface layer. This suggests a possibility of some polarization effects along boundaries of these zones if an alternating electric field is applied.

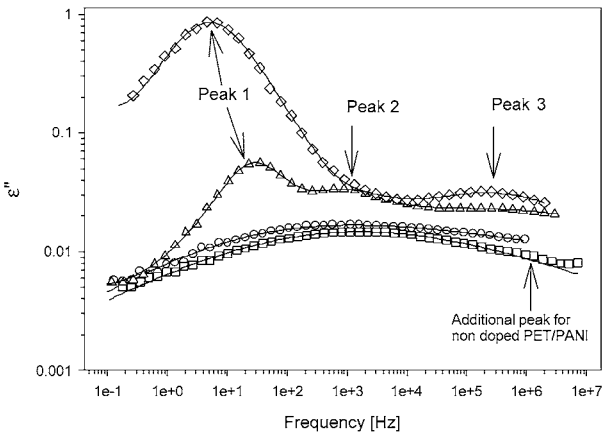

Figure 4 Dependencies of dielectric losses on frequency at 233 K for: 1—virgin PET (○); 2—PET/PANI undoped (□); 3—PET/PANI·HCl (△); 4—PET/PANI·$HClO_4$ (◇). The solid line represents the best fit to HN function.

3.2. DRS investigation

The deep changes observed on the topography of the PET/PANI composite surface under the doping effect (Figs 2 and 3) are the consequence of both charge appearance on PANI units and the penetration of counteranions into the matrix. Despite the fact that this occurs inside the very thin surface layer it changes considerably dielectric properties of the composite. Thus, the virgin PET exhibits in the investigated temperature domain a β relaxation peak, which is of large distribution (Fig. 4). The presence of the undoped PANI in the composite leads to some decrease of the relaxation strength and to the appearance of an additional not intensive relaxation process in the high frequency region (Fig. 4). The decrease of the β relaxation strength confirms probably that PANI fills the less dense volume of the PET [6] and hinders group motions.

The doping of PANI changes drastically dielectric spectra of the composite. In addition to the β relaxation, already present in the film, three other relaxation processes were revealed in the investigated temperature and frequency ranges. These new relaxation are obviously connected to the presence of charge carriers in the layer containing doped PANI as well as to the interaction between PET and doped PANI since the undoped sample revealed only one small additional high frequency relaxation at 3×10^5 Hz if compared to virgin PET. This relaxation strengthened after doping the sample to give the peak 3, probably due to the appearance of new charge carriers in the system (Fig. 4).

In order to point out the properties of the PET/PANI layer, the relative contribution of the pure PET has been retrieved from the dielectric spectra of the composite. This allowed us to fit the data with three HN relaxation functions [7]. Specifically, the low frequency peak of high amplitude (Fig. 4, peak 1) at the PET/PANI (doped by both dopants) spectra is well fitted by a Debye type function ($\alpha = 1$, $\beta = 1$) which agrees with the previous data [6]. The second relaxation process (Fig. 4, peak 2) observed in the sample doped by HCl at higher frequencies is of less magnitude and close to a Debye type ($\alpha = 0.9$, $\beta = 1$). However, in the sample doped by $HClO_4$, this relaxation is not explicit at all temperatures. Nevertheless, its presence at the high frequency side of the peak 1 is well confirmed by the asymmetry of the latter and by the corresponding HN approximation of the whole spectrum. The best fit of the peak 2 is obtained for $\alpha = 0.84$ and $\beta = 1$. The third relaxation (Fig. 4, peak 3) is distinctly observed on the spectra of the composite in the doped form. It is characterized by a large and symmetric distribution ($\alpha = 0.5$, $\beta = 1$) of relaxation times.

TABLE I Activation energies of the relaxation processes in the doped PET/PANI composite

	Activation Energy (meV)			
Sample	Peak 1	Peak2	Peak 3 (low temperatures)	Peak 3 (high temperatures)
PET/PANI·HCl	32	35	51	64
PET/PANI·$HClO_4$	40	48	33	53

The temperature dependence of the relaxation times is similar for both dopant cases. Their positions and intensities did not strongly vary with temperature as it was observed in the preliminary study [6]. However, if the first and the second relaxation peaks obey well enough the Arrhenius law with a low activation energy differing a little with the dopant used (Fig. 5, Table I), the third one shows a more complicated temperature behaviour. Specifically, two Arrhenius laws are needed to fit it correctly in the temperature range investigated and their crossover is situated at approximately 240 K (Fig. 6). This can be probably connected to an additional contribution of a new type of charge carriers inside conducting clusters.

Taking into account the two layers constituting the doped composite and the phase segregation characterizing the conducting surface layer (see the AFM part) we can suppose that the two low frequency relaxation processes exhibited by DRS spectra (peaks 1 and 2) are typical of interfacial polarization. Specifically, one of the relaxation could be understood if we consider the doped PET/PANI thin layer constituted by conducting

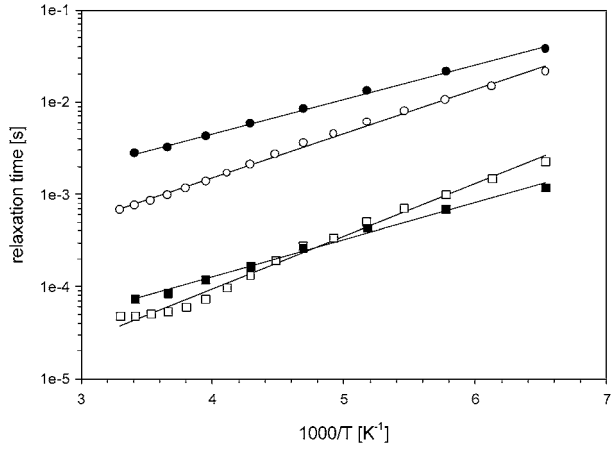

Figure 5 Arrhenius plot of the relaxation times corresponding to the peak 1 (O) and peak 2 (□) of the doped PET/PANI after subtraction of the contribution of pure Pet. The filled symbols represent PET/PANI·HCl and the empty symbols represent PET/PANI·$HClO_4$. The solid line represents the best fit to Arrhenius law.

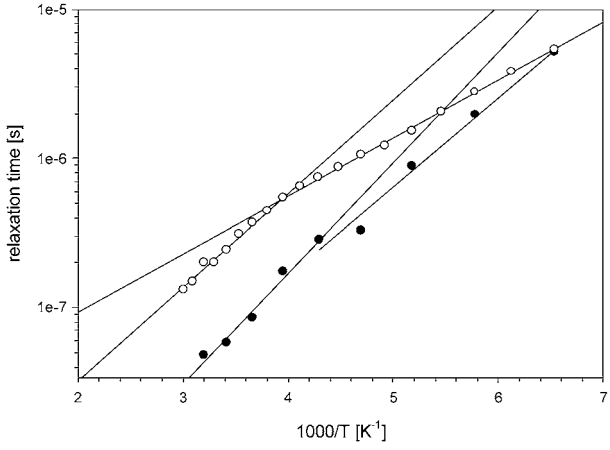

Figure 6 Temperature dependence of the high frequency relaxation process (peak 3) of the PET/PANI·$HClO_4$ (empty symbols) and PET/PANI·HCl (filled symbols). The solid line represents the best fit to Arrhenius law.

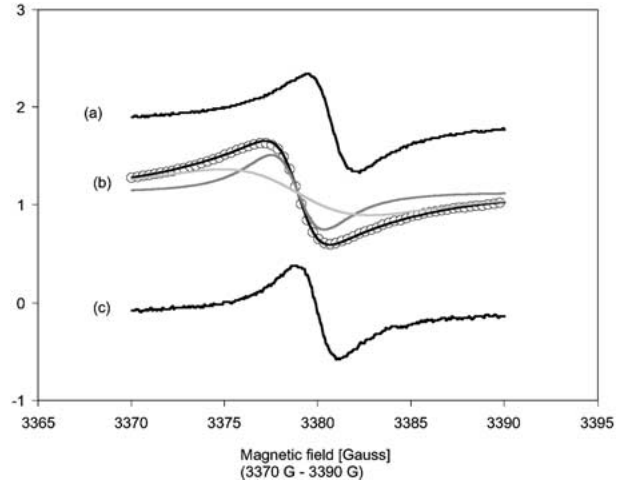

Figure 7 EPR spectra at 200 K in $HClO_4$ doped PET/PANI (a), HCl doped PET/PANI (b) and undoped sample (c). Also depicted the deconvolution of the spectrum in HCl doped sample (b).

clusters surrounded by less or non conducting medium. Such a dispersion is said to display a Debye type relaxation process and is known as the Maxwell-Wagner effect. This interpretation is conform to the conductivity distribution of the composite surface obtained by the Resiscope technique (Fig. 3). Probably, this situation is close to that of pure PANI at low and intermediate protonation levels, which is characterized by phase segregation between conducting regions and insulating background [9, 10]. The other relaxation process results from the significant difference in conductive properties between the two layers, the first one being the conducting doped PET/PANI and the second one the pure PET. This interface polarization leads also to a Debye type relaxation process. The relaxation time in both situations depends on the volume fraction of the components and is proportional to the permittivity of the insulating part and inversely proportional to the conductivity of the conducting one. Hence, as the volume fraction of the conducting layer (approximately 5–10% of the film) and the dc-conductivity do not significantly change with changing dopant, one can expect the relaxation associated to interfacial polarization between the two layers to be the same. This is the case (Fig. 5) for the second relaxation (peak 2) which is then associated to interfacial polarization between the conducting layer and the pure PET. The low frequency one (peak 1) is hence attributed to Maxwell-Wagner effect inside the conducting layer.

The relaxation peak 3 can be attributed to the conductive properties of the clusters, which exist even in the undoped composite form. This agrees with the fact that the intensity of the third relaxation increases after doping (Fig. 4). At first sight it could explain that these clusters are the ones which were present due to incomplete dedoping of the layer containing PANI. However, in that case we would observe the low frequency relaxation as it was shown for the doped samples. Therefore, the presence of charge carriers, different from those appearing in PANI due to acid doping, is more apparent. Specifically, these could be overoxidized PANI and defect sites or others [8, 9, 11]. In its turn this suggests that the intensification of the third relaxation after doping is connected to the protonation of these sites inside the clusters. Obviously, the amount of such sites is not enough high to result in a significant increase of the third relaxation (independently on the dopant).

As one can see, the relaxation behavior of the composite doped with both dopants is generally similar. However, the low frequency peak is much higher in the case of $HClO_4$ dopant. For the Maxwell-Wagner effect the dielectric strength increases with increasing the specific surface of the conducting clusters. It seems that the larger counter-anions ClO_4^- if compared to Cl^- ones induce conducting clusters of smaller size and consequently of a higher specific surface. This interpretation is conform to the conductivity distribution of the composite surface obtained by the resiscope.

3.3. EPR investigations

The presence of charge carriers in doped and undoped forms of the composite resulted in the fact that it gives EPR spectra accounted by a superposition of two Lorentzian lines (L_1 and L_2) centered at the same resonance position (Fig. 7b). However, these lines differ by their width and the thermal evolution of integrated intensities. Naturally, the latter were affected highly by the dopant presence as testified by the increase of paramagnetic charge carrier concentration. This effect probably matches the changes of dc conductivity and DRS spectra of the composite as discussed above.

3.3.1. The undoped PET/PANI composite

The EPR spectra are numerically analysed by a superposition of normalized Lorentzian lines (L1, L2) with the parameters summarized in Fig. 8a and b respectively for the integrated EPR intensity and line width. Their analysis testifies that two kinds of PC are involved and associated to $S = 1/2$-like spins in the undoped composite form. The spin susceptibility, which is proportional to the EPR line intensity, shows quite different thermal behavior. Specifically, the L1 line intensity follows a thermal evolution according to the well-known

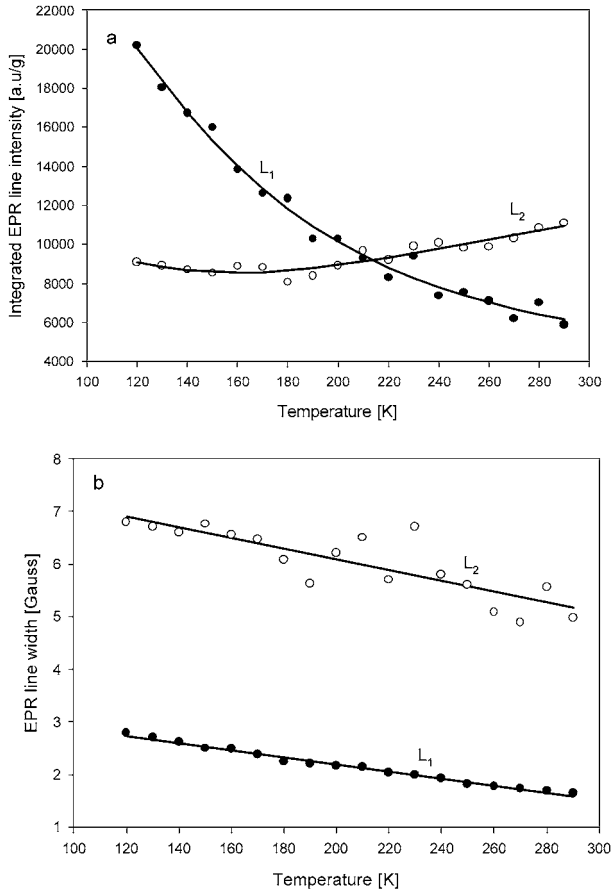

Figure 8 Integrated EPR line intensity (a) and line width (b) versus temperature in the undoped PET/PANI film. The continuous line is only a guide for eye.

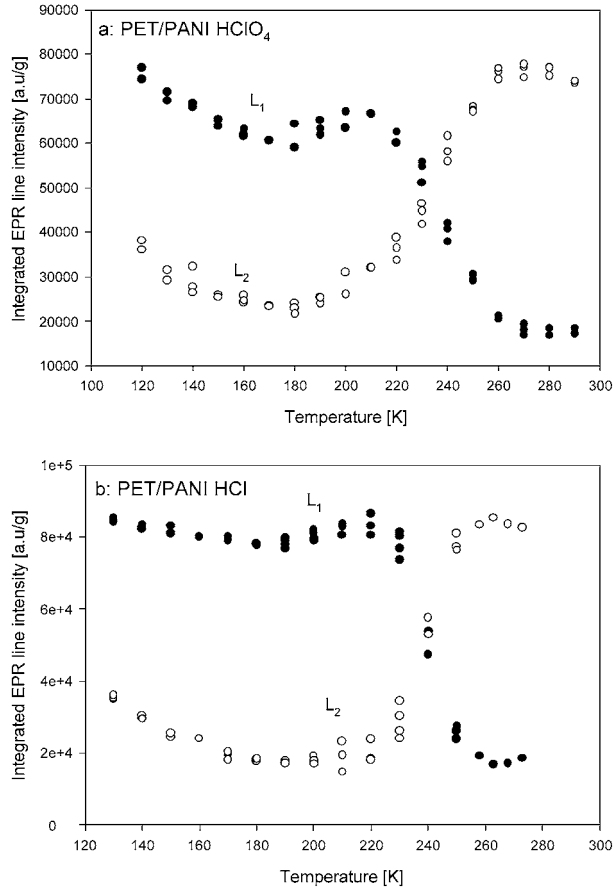

Figure 9 EPR line intensity versus temperature in PET/PANI·$HClO_4$ (a) and PET/PANI·HCl (b). The intensity scale is the same as for the undoped sample (normalised to 1 g, 10^5 amplification, 2 mw microwave power and 0.5 gauss as field modulation).

Curie law $\frac{C}{T}$ and means that we deal with localized unpaired spins (radicals or dangling bonds). The second EPR line (L2) exhibits a nearly stationary integrated intensity with the sample temperature. This behavior results from a fraction of delocalized unpaired spins giving rise to Pauli-like spin susceptibility:

$$\chi_{\mathrm{p}} = 2\mu_B^2 N(E_{\mathrm{F}})$$

where $N(E_{\mathrm{F}})$ represents the density of states at the Fermi level. Its small increase with the temperature can be related to changes of $N(E_{\mathrm{F}})$ [12–14].

The line widths for both (L_1, L_2) lines decrease smoothly when the temperature is raised (Fig. 8b). Such a behavior is obviously attributed to a decrease of the degree of PC localization because both thermal activation of the PC motions and thermally favored polymer chain librations contribute to the spin relaxation in the PET/PANI layer of the composite.

For both EPR spectrum components, the g-factor for the narrow line (L2) is 2.0032 and for the broad line (L1) is 2.0030 at room temperature. Such values are commonly reported for wide class of PC in polymer materials. The small departure from the free electron g-factor (2.0023) results from a weak spin-orbit coupling.

Taking into account the dc conductivity and DRS data we can suppose that these PC are charge carriers in the conducting clusters containing overoxidized PANI and defect sites [8, 9, 11, 15] as well as π-electron states or inter-chain charge transfer.

3.3.2. The doped PET/PANI composite

The same deconvolution process of the EPR spectra as in the case of the undoped film was applied. It appeared that the doping did not affect essentially the resonance position of the L1 and L2 lines: the PET/PANI·HCl narrow line ($g = 2.0030$) and the broad line ($g = 2.0032$); the PET/PANI·$HClO_4$ narrow line ($g = 2.0030$) and the broad line ($g = 2.0037$). We have compared the PC concentrations in doped samples to those in undoped ones. An increase by a factor 8 and 3 was found at room temperature for, respectively delocalized and localized PC independently of the used dopant. However, for both doped samples, the EPR line intensities are not only quite higher than in the case of undoped film, but exhibit different thermal behaviors (Fig. 9). From the observed susceptibility, the one (χ_1) which dominates the EPR signal at low temperature is associated to the EPR line (L1) induced by localized PC. Nevertheless, unlike the undoped composite case its intensity does not follow a thermal evolution described by the Curie law. Instead, the rapid χ_1 decrease between 200 K and 250 K is displayed. Moreover, the corresponding line width exhibits the similar thermal evolution (Fig. 10). This L1 line behavior suggests the enough fast PC transformation to be delocalized in this temperature range. Similar behaviors were reported in perchlorate doped poly(acethylene) and attributed to spin-gap-like behavior [16]. It seems this matches up to the crossover at 240 K observed for the temperature dependency of the

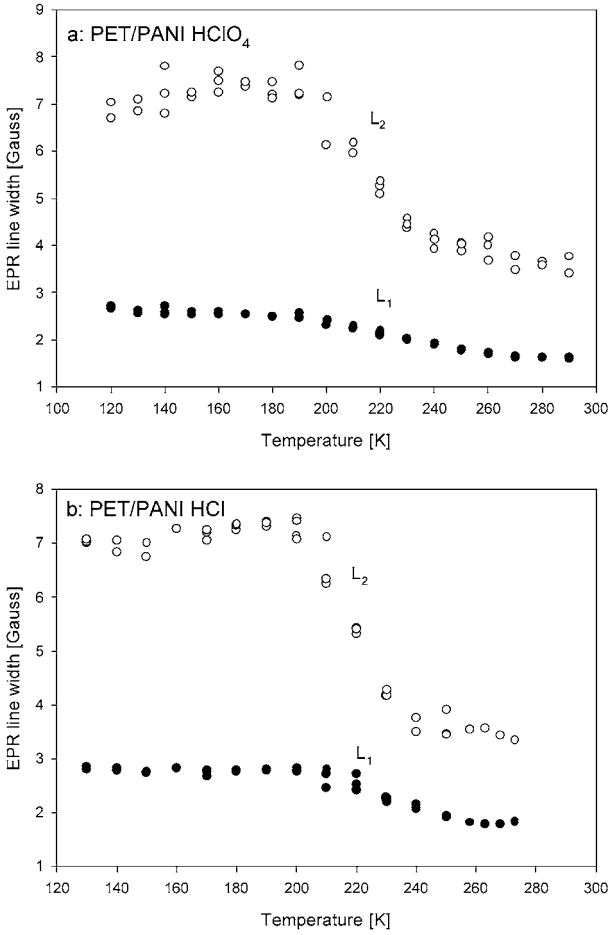

Figure 10 EPR line width versus temperature in PET/PANI·$HClO_4$ (a) and PET/PANI·HCl (b).

third peak at DRS spectra of the doped composite (see above).

The second component (L2), associated with the narrow line width, exhibits increasing intensity with temperature with an out-of-phase like behavior with respect to χ_1. Obviously, this is the mark of conversion between the localized and delocalized PC.

In both doped samples, the line widths are nearly stationary between 100 K and 180 K (Fig. 9). A decrease is observed above 180 K with the same features for both (L1) and (L2) lines. Motions thermally activated contribute to the decrease of the line widths by motional averaging process.

On the whole, the comparative EPR studies of the PET/PANI composite with and without doping point out the highly unpaired spin concentrations induced by the doping. Irrespective of the doping agent used, the thermal behavior of PC is almost the same. Delocalized paramagnetic species are induced within the temperature range 200K–250K. The electric properties which are connected with the delocalized species would exhibit similar thermal evolution with singularities in the above critical temperature range. However, if we compare this behavior with that of the undoped composite form, it can be seen that the thermal behavior anomaly of the spin susceptibility (integrated EPR line intensity) and relaxation times (inverse of line width) is caused by the dopant ions. The latter will favor the intra and interchains charge transfer which is activated by thermal energies higher than 200 K.

4. Conclusion

The data independently obtained by AFM, DRS and EPR techniques revealed the strong specificity of the PET/PANI composite, which appeared due to the irregular distribution of PANI containing conducting clusters inside the thin surface layer of the material and to a physicochemical interaction of PANI with the matrix polymer. The specificity increases after doping of the composite, which results in strong mechanical stresses heavily deforming its surface from "flat" to "mountainous". In its turn, the stresses are caused by new charge carriers and counter anions appearing in the system due to PANI protonation. Moreover, in spite of the fact that these occur inside the very thin surface layer it changes also considerably dielectric properties of the composite as a whole. This resulted in a rise of new peaks of dielectric losses on the DRS spectra, which are typical of interfacial polarization. The magnitude of the loss in low frequency range increased with the size of the counter-anion, which probably testifies to a smaller size of the formed conducting clusters and consequently to a higher specific surface. The EPR data show the presence of paramagnetic centers (PC) in both undoped and doped samples. Both localized and delocalized (PC) are evidenced and the fundamental changes concern the thermal evolution of the spin susceptibilities. Particularly, in the doped PET/PANI, the conversion between localized and delocalized (PC) is thermally activated at $T \geq 200$ K. It is interesting to emphasize the strong difference in ratios of EPR line intensities and conductivity of the undoped and doped samples. Thus, normalized EPR line intensities of the undoped PET/PANI composite are less by a factor of about 5–6 than ones of the doped samples. However, if we compare their dc conductivity, the difference is much more (by a factor of about 10^{5-6}). This difference could mean that we would have in the composite both paramagnetic and diamagnetic charge carriers. But whereas paramagnetic charge carriers with short scattering time with respect to the characteristic EPR time scale, can also exist in the conducting clusters, the EPR line intensities measured by the EPR technique in the X-band is certainly inoperative. Therefore, to judge about real nature of charge carriers it is advisable to perform measurements with EPR high wave-bands. At the same time, the data obtained unambiguously testify that the doped composite has no metallic character with regard to the behavior of the EPR line shape (no Korringa relaxation rate [17] and the absence of Dysonian-like EPR signal).

Acknowledgments

This work was partly supported in the framework of a collaboration between the Centre National de la Recherche Scientifique (CNRS) and the National Academy of Sciences (NAS) of Ukraine (project N7186). The authors would also like to thank Dr. M. Zaghrioui, LPEC, Université du Maine, Le Mans and Mr. F. Paris, Université du Maine, Le Mans, for help with dc-conductivity and 3D AFM measurements, correspondingly.

References

1. A. BHATTACHARYA and A. DE, *Progr. Solid. St. Chem.* **24** (1996) 141.
2. S. W. BYUN and S. S. IM, *Polymer* **39** (1998) 485.
3. J. ANAND, S. PALANIAPPAN and D. N. SATHYANARAYANA, *Prog. Polym. Sci.* **23** (1998) 993.
4. A. A. PUD, S. P. ROGALSKY, G. S. SHAPOVAL and A. A. KORZHENKO, *Synth. Metals* **99** (1999) 175.
5. A. A. PUD, G. S. SHAPOVAL and V. P. KUKHAR, Ukrainian claim for invention rights N94010153 of 11.05.93.
6. A. A. KORZHENKO, M. TABELLOUT, J. R. EMERY, A. A. PUD, S. P. ROGALSKY and G. S. SHAPOVAL, *Synth. Metals* **98** (1998) 157.
7. A. K. JONSCHER, "Dielectric Relaxation in Solids" (Chelsea Dielectric Press, 1996).
8. A. A. PUD, *Synth. Metals* **66** (1994) 1.
9. F. ZUO, M. ANGELOPOULOS, A. G. MACDIARMID and A. J. EPSTEIN, *Phys. Rev. B* **39** (1989) 3570.
10. H. H. S. JAVADI, K. R. CROMACK, A. G. MACDIARMID and A. J. EPSTEIN, *ibid.* **39** (1989) 3579.
11. A. G. MACDIARMID and A. J. EPSTEIN, *Faraday Discussions of the Chemical Society* **88** (1989) 317.
12. J. S. BAECK, K. S. JANG, E. J. OH and J. JOO, *Phys. Rev. B* **59** (1999) 6177.
13. R. S. KOHLMAN, J. JOO, Y. Z. WANG, J. P. POUGET, H. KANEKO, T. ISHIGURO and A. J. EPSTEIN, *Phys. Rev. Lett.* **74** (1995) 773.
14. J. M. GINDER, A. F. RICHTER, A. G. MACDIARMID and J. EPSTEIN, *Solid. State Comm.* **63** (1987) 97.
15. H. H. S. JAVADI, R. LAVERSANNE, A. J. EPSTEIN, B. K. KOHLI, E. M. SCHERR and A. G. MACDIARMID, *Synth. Metals* **29** (1989) E439.
16. T. MASUI, T. ISHIGURO and J. TSUKAMOTO, *ibid.* **104** (1999) 179.
17. J. JOO, H. G. SONG, C. K. JEONG, J. S. BAECK, J. K. LEE and K. S. RYU, *ibid.* **98** (1999) 215.

Received 31 July 2000
and accepted 1 February 2001